Earth and Planetary Science Letters 520 (2019) 212–219

Contents lists available at ScienceDirect

Earth and Planetary Science Letters

www.elsevier.com/locate/epsl

Incipient subduction at the contact with stretched continental crust: The Puysegur Trench

Michael Gurnis [a,*], Harm Van Avendonk [b], Sean P.S. Gulick [b,c], Joann Stock [a], Rupert Sutherland [d], Erin Hightower [a], Brandon Shuck [b], Jiten Patel [d], Ethan Williams [a], Dominik Kardell [b,c], Erich Herzig [a], Benjamin Idini [a], Kenny Graham [d], Justin Estep [e], Luke Carrington [f]

[a] Seismological Laboratory, California Institute of Technology, Pasadena, CA 91125, USA
[b] University of Texas Institute for Geophysics, Jackson School of Geosciences, Austin, TX 78758, USA
[c] Department of Geological Sciences, Jackson School of Geosciences, University of Texas at Austin, Austin, TX 78712, USA
[d] School of Geography, Environment and Earth Sciences, Victoria University of Wellington, Wellington 6140, New Zealand
[e] Department of Geology and Geophysics, Texas A&M University, College Station, TX 77843, USA
[f] Department of Geology, University of Otago, Dunedin, New Zealand

ARTICLE INFO

Article history:
Received 30 January 2019
Received in revised form 16 April 2019
Accepted 28 May 2019
Available online xxxx
Editor: R. Bendick

Keywords:
plate tectonics
subduction
subduction initiation
oceanic crust
oceanic lithosphere

ABSTRACT

A seismic Benioff zone and plate kinematics show Puysegur Trench south of New Zealand transitioning to subduction. Because the local structure and its influence on subduction initiation is poorly understood, we conducted a seismic survey with ocean bottom seismometers and multichannel seismic profiles. Our early results show that the overriding Pacific Plate beneath the Solander Basin is composed of block-faulted and thinned continental crust, and the inner trench wall of northern Puysegur Ridge is composed of folded and faulted sediment. The megathrust interface has been imaged and shows ~500 m of downgoing, undisturbed sediments. Combining plate kinematic history with seismic velocity-inferred density, we show that the density difference across the plate boundary changed as oblique strike-slip plate motion juxtaposed dense oceanic crust with thinned continental crust. The density difference rapidly increased 18 to 15 Ma, coincident with subduction initiation, suggesting that compositional differences have a large influence on subduction initiation.

© 2019 Elsevier B.V. All rights reserved.

1. Introduction

Interpretation of Cenozoic Pacific Plate kinematics and theoretical investigations suggest that the balance of forces on plates is changed by subduction initiation (Gurnis et al., 2004; Stern and Bloomer, 1992). In order to make substantial strides in understanding the dynamics of plate motions, specifically the forces that drive and resist oceanic plates, we need a detailed framework of early subduction evolution, including a picture of the nucleation stage. Many studies have examined the geological rock record of young or mature arc systems, but well-developed arcs do not preserve evidence of their early evolution, and ephemeral properties (e.g. stress state) are particularly poorly recorded. Consequently, the dynamics and details of subduction initiation remain obscure. Of particular interest are the stresses operating at a nascent boundary, tectonic requirements for the initiation process, and material properties of the interface and adjacent plates as initiation proceeds (Gurnis et al., 2004; McKenzie, 1977; Nikolaeva et al., 2010; Reagan et al., 2017; Stern, 2004; Toth and Gurnis, 1998).

A key unknown in subduction initiation is what controls the transition to a self-sustaining state, in which the negative buoyancy of downgoing oceanic lithosphere exceeds the resisting force associated with fault friction, plate bending, and other resistive processes (McKenzie, 1977; Toth and Gurnis, 1998). The transition may require weakening of the plate interface through grain-scale processes (Thielmann and Kaus, 2012), the addition of fluids or sediments (Dymkova and Gerya, 2013), or augmentation of thermal buoyancy with compositional differences between tectonic elements (Leng and Gurnis, 2015; Nikolaeva et al., 2010); new plate boundary defining faults may form from or adjacent to pre-existing faults (Mao et al., 2017). The critical evidence to address these issues can be assembled by investigating a subduction zone that has partially proceeded through the nucleation stage. Analyzing such a young subduction zone allows for accurate plate kinematics, along with detailed knowledge of both the tecton-

* Corresponding author.
E-mail address: gurnis@gps.caltech.edu (M. Gurnis).

https://doi.org/10.1016/j.epsl.2019.05.044
0012-821X/© 2019 Elsevier B.V. All rights reserved.

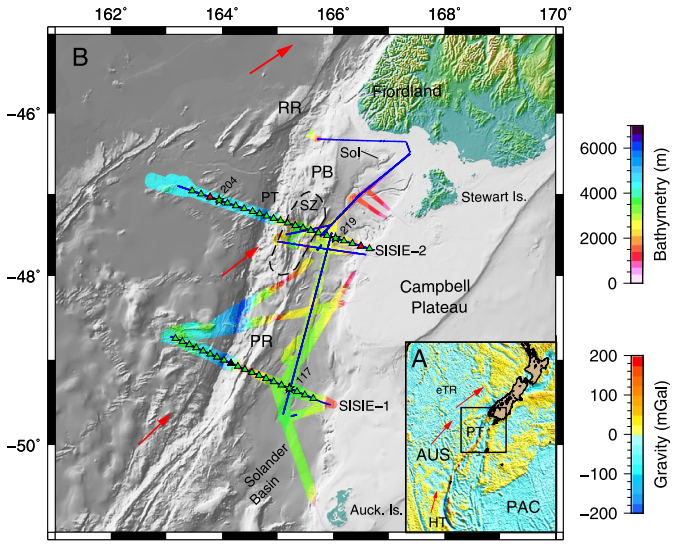

Fig. 1. A. Puysegur study region (black rectangle). The Macquarie Ridge Complex is the long narrow gravity high/low feature between the Hjort Trench (HT) and the Puysegur Trench (PT). The Extinct Tasman Ridge is eTR. Base map is free-air gravity (Sandwell and Smith, 1997). B. Bathymetry of Puysegur Ridge (PR) and Trench region. Background gray scale is from NIWA (Mitchell et al., 2012) while the bathymetry acquired during MGL1803 is overlain in color. MCS lines acquired shown as solid blue lines. Symbols for OBS include those used for velocity and density (stars, labeled), all others with quality data (green triangles), one that was not recovered (black triangle) and those with unusable data (red triangles). The combined OBS/MCS lines are labeled as SISIE-1 and SISIE-2. The Snares Zone (SZ) is outlined with a black dashed line, Resolution Ridge is labeled as RR, Solander Island as Sol and Puysegur Bank as PB. In A and B, red arrows are the modern relative plate motion (DeMets et al., 2010) of AUS (or Macquarie Plate) with respect to PAC. (For interpretation of the colors in the figure(s), the reader is referred to the web version of this article.)

ics that precede nucleation and the history during nucleation, to constrain subduction initiation. Although there are well-known examples where subduction initiated and then evolved into systems with self-sustaining forces, such as initiation of Izu-Bonin-Marianas (IBM) in the Eocene (Arculus et al., 2015; Ishizuka et al., 2006; Stern and Bloomer, 1992), the evolution of the resulting arc has overprinted much of the record of initiation dynamics. Likewise, more mature arc-trench systems are too ambiguous to be reliably used. Some potentially incipient subduction zones, on the other hand, are sufficiently young (Mussau Trench, the Owen Ridge, Gorringe Bank) that slab bending in the hinge zone may not have begun (Gurnis et al., 2004).

The Puysegur Trench south of New Zealand, an incipient subduction zone, overcomes these limitations: known plate motions and earlier geophysical surveys show that the Puysegur Trench is at the necessary intermediate stage of transitioning to self-sustaining subduction. Accurate constraints on plate tectonics together with numerous earthquakes show the conversion from strike-slip kinematics along the Macquarie Ridge in the south, to a well resolved seismic Benioff zone underneath Fiordland (Fig. S1), in the southwestern corner of the South Island (Fig. 1), in the north. The Puysegur-Fiordland system is a subduction zone with plate convergence, a trench, a seismic Benioff zone down to nearly 150 km depth (Eberhart-Philips and Reyners, 2001), and sparse, young calc-alkaline volcanism in the overriding Pacific Plate (Mortimer et al., 2013). The Fiordland slab appears to have a "plowshare" shape caused by oblique convergence into the mantle (Christoffel and van der Linden, 1972).

2. The Puysegur boundary

Relative motion between the Australian (AUS) and Pacific (PAC) plates since the Eocene is well known (Cande and Stock, 2004). The Puysegur-Fiordland subduction zone is at the northern end of the Macquarie Ridge Complex (MRC), defining the AUS-PAC plate margin. South to north, the MRC is characterized by narrow, long gravity and bathymetry highs alongside lows from the Hjort Trench to the Puysegur Trench and Ridge (Hayes and Talwani, 1972; Sutherland, 1995; Walcott, 1998) (Fig. 1A). Present plate motion is dextral strike-slip with oblique convergence beneath Puysegur Ridge and Fiordland. The Tasman Sea (eTR, Fig. 1A) ceased spreading at ∼52 Ma, followed by a new interval of sea floor spreading along the Pacific-Australia margin starting at ∼45 Ma. Rifting was initially perpendicular to the conjugate margins (e.g., Resolution Ridge on the Australian plate and the western edge of the Campbell Plateau; Fig. 1B) but became increasingly more oblique (Fig. 2) due to the migration of the AUS-PAC pole of rotation southward during the Miocene (Sutherland, 1995; Walcott, 1998). This motion produced characteristic fracture zones (FZ) that curve and merge along the MRC and that are evident in satellite gravity and swath bathymetry on both plates (Delteil et al., 1996; Lamarche and Lebrun, 2000; Massell et al., 2000). Abyssal hills are generally perpendicular to the FZs (Fig. 1B) (Lamarche et al., 1997). The along-strike variations in FZ orientation and the fabric of abyssal hills along the MRC have been used to infer under-thrusting of the Australian Plate beneath the Pacific Plate along the Hjort and Macquarie sectors (Massell et al., 2000; Meckel et al., 2003). A distinct bend in the orientation of the MRC begins at the Puysegur segment (Fig. 1A), where oblique convergence is evident from modern relative plate motions (Sutherland et al., 2000). Relative plate motion was mostly strike-slip after ∼10 Ma, with convergence at the position of the Puysegur Trench. The exact time and geometry by which PAC-AUS spreading ceased is not well known because the obliquity of the available ship tracks to the numerous closely spaced fracture zones complicates interpretation of magnetic anomalies. There are ages as young as 8–9 Ma at Macquarie Island much further to the south (Portner et al., 2011; Quilty et al., 2008), but whether these represent lavas erupted during slow spreading at Macquarie Island much farther to the south, but it is unclear if these ages represent lavas erupted during slow spreading, or minor volcanism on a fossil ridge. Nevertheless, 600 km of strike-slip displacement and 150–200 km of convergence have occurred since 20 Ma (Sutherland et al., 2006). By unfolding the Benioff zone beneath Fiordland about its local strike (Sutherland et al., 2006), the present slab must have underthrust the northern edge of the Fiordland crust between 16 and 10 Ma, Solander Island between 11 and 8 Ma, and southernmost Puysegur Ridge since several million years ago. The transpressional environment much farther south at Macquarie Island, with continuing volcanism until 9 Ma, does not preclude subduction initiation farther north along the plate boundary, in the Puysegur region, prior to 9 Ma.

Crustal structure and tectonic interactions related to the above AUS-PAC kinematic history have not yet been determined with much accuracy. Starting from the north, Fiordland (Fig. 1B) has granulite facies rocks exposed at the surface and produced in a convergent margin with collision and accretion of arc material from the Jurassic to the Early Cretaceous (Clarke et al., 2000). Fiordland is thought to be the root of a Cretaceous arc (Davey, 2005), although its crustal thickness is poorly known and perhaps relatively thin. It is immediately underlain by a high seismic velocity slab of the subducting Australian Plate (Eberhart-Philips and Reyners, 2001). During the Miocene, Fiordland experienced several km of rock uplift, putatively in response to subduction initiation (House et al., 2002; Sutherland et al., 2009). Beneath the continental shelf near Stewart Island, the crust may be as thick as 30 km, but the Moho shallows to 20 km in the northern Solander Basin (Melhuish et al., 1999).

Sections of the Puysegur convergent margin have been theorized to represent forced and self-sustaining stages of subduction

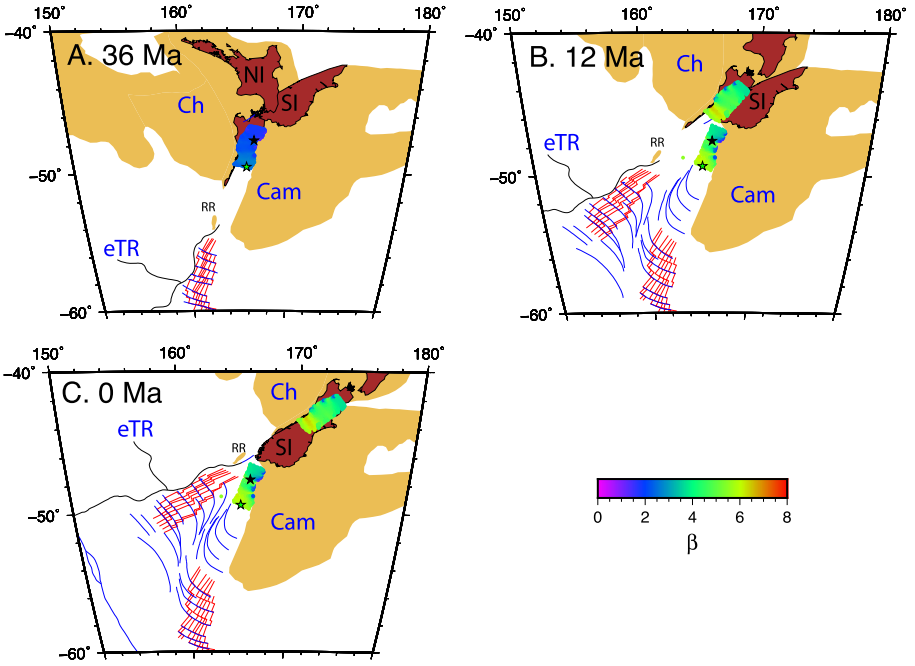

Fig. 2. Generalized reconstruction in PAC frame of reference at 36 Ma (A), 12 Ma (B) and the present (C) using rotations for Australia-Pacific computed using the Pacific-West Antarctica rotations of Croon et al. (2008) and the composite West Antarctica-East Antarctica-Australia rotations of Granot and Dyment (2018). Fracture zones and magnetic lineations from Keller (2003). Stretching factors, β (final width divided by initial width of a block of crust) are color coded, within the Solander Basin and its conjugate using the deforming plate methods in GPlates (Gurnis et al., 2018) using only stretching implied by finite rotations; no post rifting deformation tracked. Green star is position of OBS 117 and black star OBS 219. Labels are: South Island (SI), North Island (NI), Campbell Plateau (Cam), Challenger Plateau (Ch), Resolution Ridge (RR), and extinct Tasman Ridge (eTR).

(Gurnis et al., 2004), but prior to our study, adequate seismic reflection images of the crustal structure did not yet exist south of 47°S. The Puysegur Ridge has been hypothesized to be oceanic crust (Delteil et al., 1996) similar to Macquarie Island to the south. A seismic reflection line acquired by R/V Maurice Ewing in 1995 found a shallow (~20 km depth) Moho, and evidence for Miocene fault re-activation (Sutherland and Melhuish, 2000). It is unclear on which structure subduction nucleated, either through reorientation of a fracture zone or through formation of an entirely new fault (Collot et al., 1995). There are large amplitude gravity anomalies (Lebrun et al., 1998) with poorly constrained structural interpretations along the Puysegur Ridge. The crustal structure of the region remains unknown, so the density differences that existed when subduction initiated remain poorly known.

3. New data and results

We undertook marine geophysical survey MGL1803 of the Puysegur subduction zone in February-March 2018 using R/V Marcus G. Langseth. This project was entitled the South Island Subduction Initiation Experiment (SISIE). Seismic reflection and refraction data were acquired to 50°S (Fig. 1) with a large acoustic source (108 l, ~6600 in^3). For multichannel seismic (MCS) imaging, the vessel towed a streamer either 4.05 or 12.6 km long, weather dependent. The longer streamer provided opportunities to suppress seafloor multiple energy that interferes with crustal targets and allowed for better estimation of stacking velocities. We acquired 717 km of MCS data using the 12.6 km streamer and 535 km using the 4.05 km streamer, with a 50 m shot interval and ~22 s records. A group of 28 ocean-bottom seismometers (OBSs) from the University of Texas Institute of Geophysics (UTIG) occupied 43 sites on two refraction lines. The two east-west OBS lines across Puysegur Trench were shot with a 150 m shot interval and ~60 s records to avoid noise from previous shots. Seismic data were obtained from 39 of 42 OBS; one OBS was not recovered. We also successfully acquired multibeam swath bathymetry, chirp subbottom profiler, gravity and magnetometer data.

Initial processing of the MCS data included trace editing, noise attenuation, bandpass filtering, trace balancing, spherical divergence correction, normal moveout correction following velocity analysis, multiple suppression, inside and outside muting, and stacking. These initially processed data were then Kirchhoff time migrated and the OBS and MCS data were integrated by converting the OBS velocity model into two-way travel time. The OBS-derived velocity model was used to convert the interpreted horizons (Fig. 3A, C) to depth (Fig. 3B, D).

Preliminary post-stack time-migrated MCS images (Figs. 4–7, S2) confirm that the incoming Australian Plate is only thinly sedimented, but the Pacific Plate has thick (>1 km) sediment cover. Between the Australian Plate and Solander Basin lies Puysegur Ridge, which is sediment free in the south (Fig. 3) but overlain by thick layers of moderately to highly deformed sediments in the north (Fig. 3A, B). Extensive sediment cover on the northern Puysegur Ridge was unexpected (Delteil et al., 1996). For the east-west MCS/OBS lines, SISIE-1 in the south and SISIE-2 in the north, we made preliminary picks of seafloor, basement, the décollement between subducting and overriding plates, and sedimentary layers (Fig. 3).

The incoming Australian Plate is rough and highly faulted with small, isolated pockets of sediment with thickness <500 m. Basement relief is up to 1 km over distances <10 km and associated with abyssal hill fabric (Fig. 1B). This morphology is consistent with oceanic crust generated at a slow spreading center (Reston et al., 1996). On the subducting Australian Plate, the thickest sediment occurs within the Puysegur Trench on the northern profile (1 km, Fig. 3B). Sediments within the trench are mostly undeformed but have indications of potential reverse faulting at the base of the section in the eastern half of the trench and beneath the décollement.

The décollement between the subducting and overriding plates is evident in seismic reflection images of SISIE Lines 1 and 2.

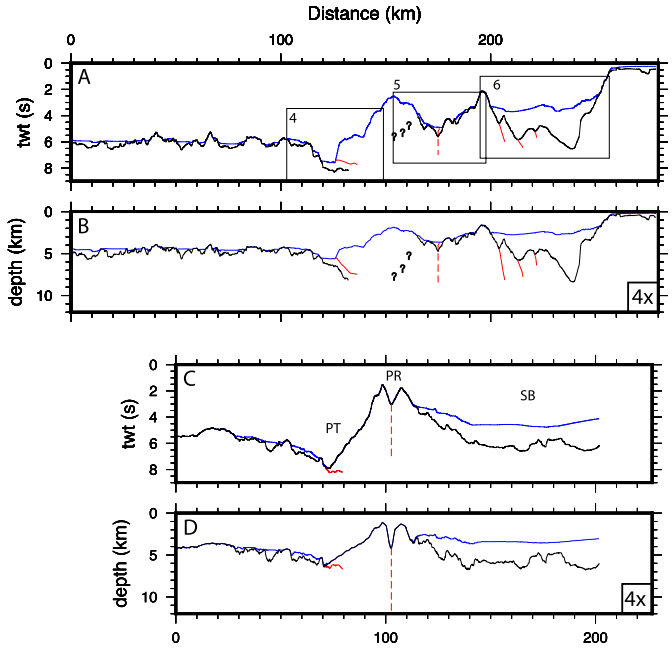

Fig. 3. A. Line drawing of the northern line SISIE-2, shown with basement contact (black), top of the sediments at the sea floor (blue), décollement and faults between crustal blocks (red), and question marks where location of basement below the sediments is uncertain. The locations of detailed MCS images for three regions are shown by black boxes labeled with the Figure number 4, 5 and 6. B. Depth converted section for SISIE-2. The vertical exaggeration 4× is indicated. Line colors as in A. C. As A, except for SISIE-1. D. Same as B, except for SISIE-1. See Fig. 1B for location of the SISIE-1 and -2 lines. Throughout, the vertical dashed red lines are interpreted strike slip faults.

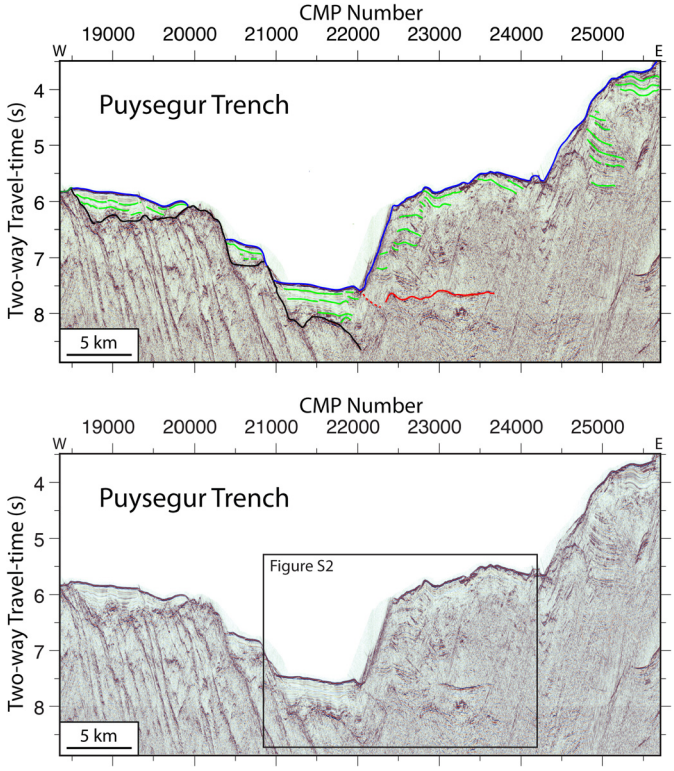

Fig. 4. Details for the interpretation of the Puysegur Trench from SISIE-2; see Fig. 1B for location of SISIE-2. The top panel shows interpretation of time-migrated multichannel seismic line for the Puysegur Trench and the western side of the Puysegur Ridge. Interpretations are more schematic than complete interpretation of all horizons and faults. Lines indicate: top of sediments (blue), basement (black), sedimentary horizons (green), and décollement (red, dashed where uncertain). The bottom panel shows the uninterpreted MCS image. Outline of the detailed images of the décollement shown in Fig. S2. For upper part of section V.E. ∼4:1 @ 2 km/s.

Along the northern profile (Line 2), the décollement separates deformed sedimentary strata of western Puysegur Ridge (adjacent to the Snares Zone) from sediments on the incoming Australian Plate (Figs. 3A, B, S2), and dips at roughly 15°. On the southern line, the contact lies between basement rock and a thin subducting layer of sediment and is close to horizontal (Fig. 3D). The décollement detected at these two positions is consistent with the location and focal mechanisms of earthquake inferred from global seismic networks (Fig. S1).

The sediments are thicker of more variable thickness in the Solander Basin. On the northern line, sediment thickness is up to 6 km, but typically 2–3 km. On the southern line, thickness was more uniform at 2–3 km. Sedimentary structures within Solander Basin reflect submarine depositional settings: onlap surfaces at basin edges and channel/levee deposits associated with north to south transport (Schuur et al., 1998). The sediments appear to be primarily post-rift sediments, but further analysis of all of the lines may uncover syn-rift sediments. The basement surface along SISIE-1 has low relief of 1–2 km, as compared to up to 5 km for SISIE-2. On the northern line, there are tilted block-faulted structures each with moderate dip angle (between 35° to 55°) detachment surfaces (Figs. 3A, B, 6). Undeformed sediments overlie block faulted structures, indicating that crustal faults were inactive during the majority of basin filling.

Puysegur Ridge has substantial along-strike differences in character. The Snares Zone (Fig. 5), is a local depression, in places sediment filled (∼1 km), of Puysegur Ridge that is dissected by strike-slip faulting and has deep (>1000 m) wave-cut surfaces indicating subsidence from sea level. Within the central depression of the Snares Zone, at about CMP 30000, the MCS data show a vertical fault adjacent to a sharp fold, that dissects otherwise flat-lying sediments (Fig. 5). A unique interpretation is not possible, but we interpret this feature as a strike-slip fault (Fig. 3A, B). Along the west flank of Puysegur Ridge (Figs. 4, S2), a large structure composed of deformed sediments, more than 10 km in width and about 3 km in depth, was imaged (east of 24250 CMP, Fig. 4). There are folded sedimentary layers on the western half of this block that are potentially truncated by thrust faults from the seafloor to the décollement, but identifying individual faults with clear offset is difficult on these sections and will be a target of additional processing. For the eastern half of this block, layered sediments are identified to 0.75 s TWT below the sea floor and we cannot determine the location of the décollement locally. At 24,250 CMP, there is an abrupt shoaling and deformed sediments within the upper ∼1.5 s TWT can be identified. Below 5.7 s TWT, we cannot yet determine if the material is sediment. The southern profile has a ridge and trench-facing slope that is covered by only a thin layer of sediment. The interior trough at the ridge summit on the southern profile is assumed to be where the trace of the main strike slip fault lies (Collot et al., 1995) and is also nearly sediment free.

We use seismic refractions recorded on three OBSs (Fig. 7A–C) to infer the first-order crustal structure. First, we calculated ray paths for first-arriving phases between the airgun shots and instruments for 1-D seismic velocity models beneath the 2-D bathymetry. We selected the best-fitting 1-D model for each seismic station by minimizing the average travel-time misfit. Vertical seismic velocity profiles are shown for OBS 204 (Australian Plate), OBS 117 (southern Solander Basin), and OBS 219 (northern Solander Basin) (Fig. 8). The three instruments recorded refractions turning in sediments, crust and upper mantle, respectively, at offsets up to 70 km. Site 204 has a crustal thickness of approximately 7 km, which is within the range of normal oceanic crust (Van Avendonk et al., 2017). Sites 117 and 219 have seismic wave speeds lower than that of oceanic crust, consistent with rifted mar-

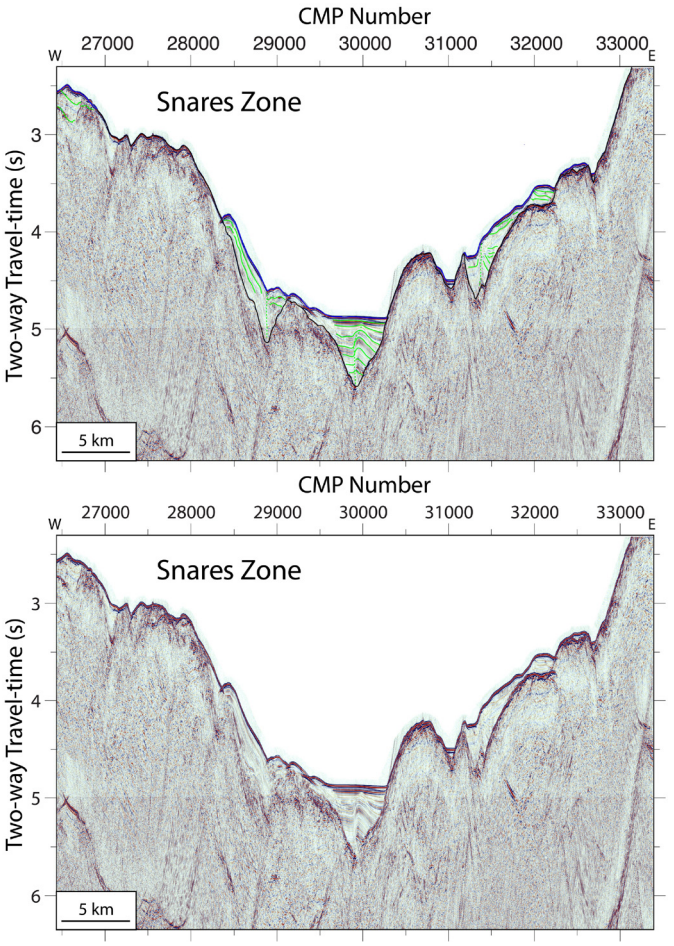

Fig. 5. Same as Fig. 4, except for the Snares Zone. An interpreted nearly vertical strike-slip fault is denoted as a green dashed line. For upper part of section V.E. ~4:1 @ 2 km/s.

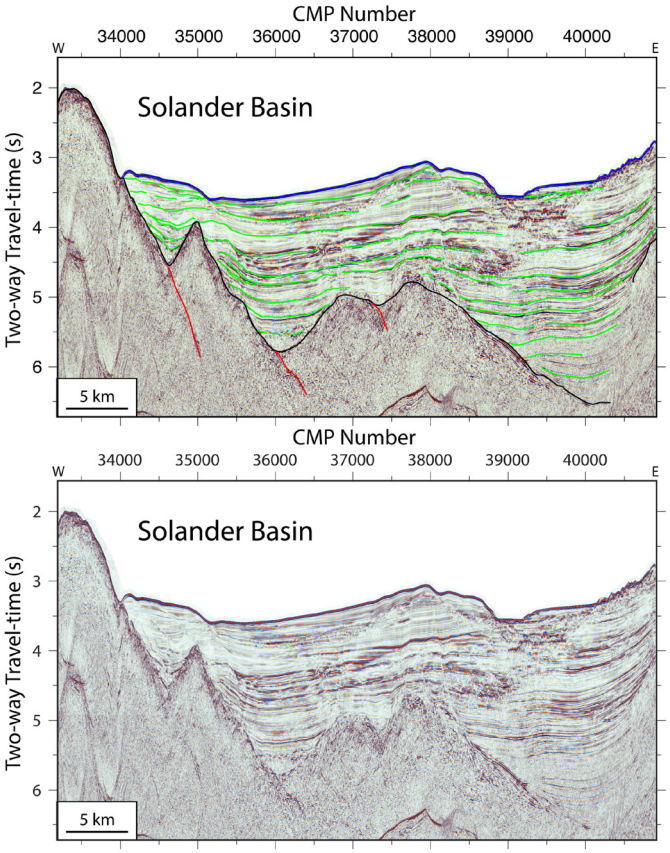

Fig. 6. Same as Fig. 4, except for the Solander Basin along SISIE-2 line. Interpreted faults in basement shown in red. For upper part of section V.E. ~4:1 @ 2 km/s. For depths for basement with faults V.E. ~2:1 @ 4 km/s.

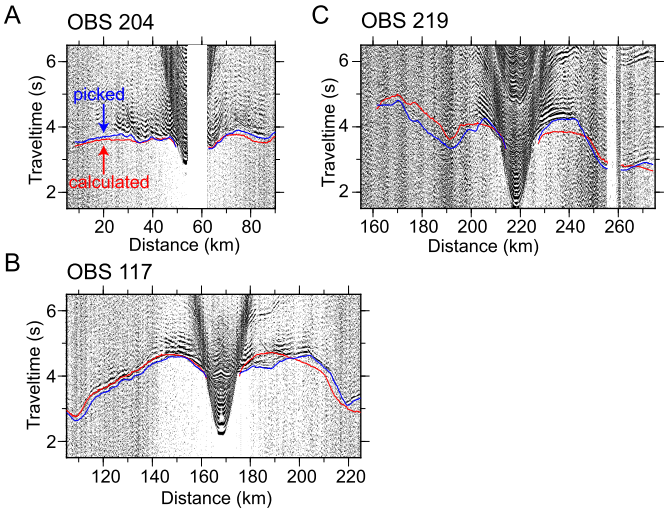

Fig. 7. Seismic refraction data and interpretations for (A) OBS 204, (B) OBS 117 and (C) OBS 219. Picked arrivals are in blue and computed from 1-D model (Fig. 8) in red. The reduction velocity used in the figures is 7 km/s.

gin crust (Klingelhoefer et al., 2016), but the crust is thicker to the north, and less extended.

4. Discussion and conclusions

Our results have significant implications for understanding the conditions required for subduction initiation. Puysegur tectonics has been viewed as an example of induced subduction initiation through transpression along a former spreading and fracture zone system with ocean crust, with continental crust playing no role and sediments only playing a small role (Collot et al., 1995; Gurnis et al., 2004). The new observations show that continental crust actually played a significant role in the evolution of the plate boundary. The overriding plate is not oceanic in nature along much of the plate boundary where subduction initiated but is instead block-faulted and extended continental crust. The density contrast between the converging plates is likely to be significant. In addition, we image subducted and accreted sediment near the décollement, raising the possibility that elevated fluid pressure from sediment dewatering may have lowered effective stress at the newly-developing plate interface.

Within the earlier published framework of Puysegur subduction, initiation nucleated near a recently shut-down spreading center (Collot et al., 1995) with essentially no substantial density difference across the margin. However, isostatic arguments (Niu et al., 2003) and geodynamic models (Leng and Gurnis, 2015; Nikolaeva et al., 2010) suggest the importance of compositional density contrasts during subduction initiation. Models have shown for systems without compression that the combined density differences from both thermal structure associated with differences in plate age, as well as compositional differences from a thicker continental crust versus thinner oceanic crust, could be sufficient to drive subduction initiation (Leng and Gurnis, 2015). Along the Puysegur margin, these conditions are not entirely met as plate reconstructions do not predict a large age contrast between the Australian and Pacific Plates during evolution from divergence to

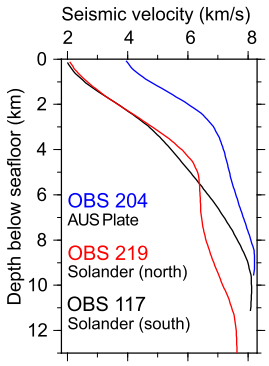

Fig. 8. Three 1-D seismic velocity profiles derived from OBS records for OBS 117, 204 and 219.

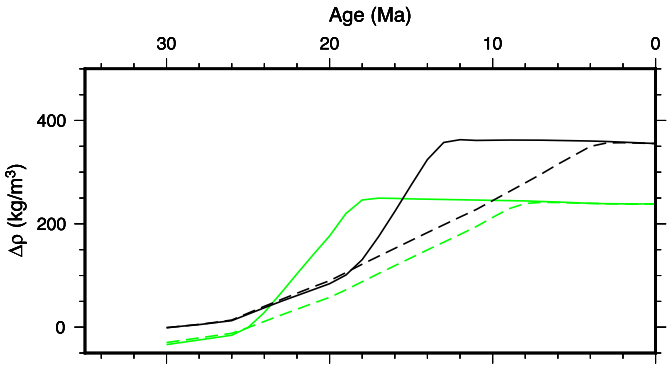

Fig. 9. The computed density differences across the Puysegur margin are shown as a function of time using the plate reconstruction shown in Fig. 2. Two large sources of uncertainty in the estimate are considered, the latitude at which the estimate is made and the density of the Solander Basin (and its conjugate) south of the survey area. We estimate the density differences at the position of OBSs 117 and 219 shown in green and black respectively. Crustal structure south of SISIE-1 is poorly known. Crustal density is assumed to vary linearly from the stretched continental crust at SISIE-1 to oceanic crust (similar to that measured at OBS 204) 500 km to the south (dashed lines) or more abruptly over 200 km (solid lines).

transpression (Fig. 2A–C). Puysegur Trench abuts continental crust north of 47°S and the onshore component of the subduction zone, Fiordland, is the root of a Cretaceous arc (Davey, 2005). Through the southern part of South Island, a suite of intrusions contiguous with Fiordland forms the Median Batholith (Davey, 2005; Mortimer et al., 1999). The overall EW-trending tectonic fabric in South Island progressively rotates clockwise closer to Fiordland and the Alpine fault. Following these structural trends, southward extrapolation of the features seen on N-S seismic lines suggests that this paleo-subduction zone could underlie Solander Basin.

The Puysegur subduction zone nucleated where compositional differences existed, and these could have played a significant role in the initiation process. The seismic velocity structure suggests a density contrast across the Puysegur region: seismic velocities of the Australian Plate are typical of slow-spreading oceanic crust, and at 7 km the thickness is just 1–2 km greater than average (Van Avendonk et al., 2017), while those within Solander Basin are typical of rifted continental crust with sediment cover (Klingelhoefer et al., 2016). Sediment thickness in Solander Basin can account for most of the difference in shallow structure, but the vertical seismic velocity gradient in the Australian Plate crust is clearly larger than in the Pacific crust profiles (Fig. 8). There is also a difference in crustal seismic velocity from north to south within Solander Basin: substantially lower velocities are modeled for the northern SISIE-2 line, as compared to SISIE-1. Seismic velocities are mapped into preliminary density profiles using the Nafe-Drake V_p–ρ relationship (with the (Brocher, 2005) regression using the data compilation of Ludwig et al. (1970)). When V_p is interpolated down to 13 km depth, we find that the average density of the incoming Australian plate is 3,080 kg/m^3, the northern Solander Basin is 2,730 kg/m^3, and the southern Solander Basin is 2,840 kg/m^3.

We estimate the density difference between the Australian and Pacific plates as a function of geologic age by combining a plate reconstruction (Fig. 2, see caption for details) with our seismically-inferred present day density profiles. By tracking how crustal blocks of different densities moved past one another, we estimate the density difference across the margin (Fig. 9; see caption for details). We suggest that in the region of Puysegur Ridge from 40 Ma to 30 Ma there was no density difference as the plates diverged and crustal thinning created Solander Basin. We assume that extension did not lead to seafloor spreading in the intra-continental rift between Campbell Plateau and its conjugate Challenger Plateau margin (Fig. 2). The transition to fully oceanic crust lies south of the SISIE-1 line on the Pacific Plate. Starting at about 30 Ma, thin continental crust of the Australian Plate moved northward relative to the Pacific Plate and was separated from conjugate thin crust of Solander Basin. There was an increase in density contrast across the plate boundary after 24 Ma at southern Solander Basin and after 18 Ma at northern Solander Basin (Fig. 9). By 15 Ma, the density difference would have reached its maximum of 350 kg/m^3, which was sustained to the present day. The estimated jump in density could have occurred as early as 20 Ma if we assumed the density difference between OBS 117 and the Australian plate (Fig. 9). The inferred age of subduction initiation is 15–12 Ma, based on the time required to backtrack the bottom of the Fiordland slab to Puysegur Trench (Sutherland et al., 2006). We propose that the correlation between this unfolded-slab-kinematic age and the time when maximum density difference was achieved is strong evidence that the juxtaposition of different materials allowed induced initiation of a discrete subduction zone, rather than development of a complex zone of inter-plate deformation. Refined analysis based on two dimensional analysis of the seismic refraction lines, as well as 3D gravity modeling of this structure merged with additional MCS lines (Fig. 1B), will likely lead to more formal bounds on the estimated density difference, and could corroborate the overall conclusion that there was a jump in the density difference across the Puysegur margin as the Solander Basin conjugate translated to the north (Fig. 2).

Basement roughness on MCS profile SISIE-2 through the northern Solander Basin (CMP 34,500 to 35,500, Fig. 6) is reminiscent of a faulted magma-poor margin (e.g., McIntosh et al., 2014; Reston and Pérez-Gussinyé, 2007). We infer that Eocene continental breakup between the western Campbell Plateau of the Pacific Plate and Challenger Plateau of the Australian Plate (Sutherland, 1995) left a ~100 km wide section of stretched and thinned continental crust in the northern Solander Basin. We interpret the 2–4 km basement relief as caused by extensional faults, though the total extension may be greater than the sum of fault offsets visible in MCS images (McDermott and Reston, 2015). If faults at the Campbell Plateau margin cut the Moho, as they do in central Solander Basin (Sutherland and Melhuish, 2000), rifting may have resulted in hydration of uppermost continental mantle. We do not yet know if seismic velocities beneath Solander Basin are consistent with this scenario, but the low strength of serpentine (Escartin et al., 1997) could play an important role in the subduction initiation process. In our reconstruction, there is a 10 Myr period during opening of Solander Basin (Fig. 2) that could allow faults and upper mantle to become serpentinized.

At the northern SISIE-2 line, we image subducting sediment, and a significant accumulation of deformed sediment to the overriding plate (>1 km thickness). It is possible that fluid expulsion during deformation and tectonic burial affected pore fluid pressure at the evolving subduction interface. We do not know the age of this sediment; it may predate subduction initiation, or have

been accreted during oblique convergence. At a convergence velocity of 1 cm/yr, it would take ∼5 Myr to build the observed accumulation, based on the observed incoming sediment thickness. However, care must be exercised as there is little sediment in the trench along our southern line, and there may have been tectonic transport of trench slope material northward by oblique subduction (e.g. Malatesta et al., 2013). Subduction initiated at 15–12 Ma, so sediment accumulation by accretion could be consistent with the duration of subduction, and would suggest that accretion resulted in progressive weakening of the subduction thrust as fluid pressure within the fault increased with time. Alternatively, the deformed sediment we image could pre-date subduction initiation. Thick (>2 km) sediment is imaged beneath Puysegur Bank, northeast of the Snares Zone, and is inferred from dredge samples and correlation to the Solander-1 and Parara-1 wells to be of Eocene-Miocene age (Sutherland et al., 2006). If subduction initiation exploited a pre-existing fault in the Snares Zone, then it may already have had a thick sediment accumulation adjacent to it, and these sediments may have then been incorporated into the zone at a very early stage. Determination of the age of deformed sediments of the trench slope by future direct sampling could provide important constraints on what happened during the nucleation phase of subduction initiation.

The SISIE results show that the Puysegur subduction zone may have nucleated at the boundary of a fault-bounded block of thinned continental crust, but the faults detected in the Solander Basin are high angle (estimated dips are between 35° and 55°) and the new plate boundary, the décollement, is close to horizontal at SISIE-1 and about 10°–15° at SISIE-2. Whether a higher angle crustal fault rotated to become the décollement or whether a new fault formed as suggested by conceptual (Collot et al., 1995) and computational models (Mao et al., 2017) for Puysegur initiation – both assuming oceanic lithosphere and crust on both sides of the trench – is not yet clear, but analysis of the sediments in the inner trench wall, through further investigation of the seismic images via direct sampling and additional processing, could help to resolve this issue.

With Puysegur having oceanic crust adjacent to continental, there may be no confirmed examples of subduction initiation at normal oceanic crust juxtaposed against normal oceanic crust. It appears that Izu-Bonin-Marianas subduction initiated at a relic Mesozoic island arc (Leng and Gurnis, 2015), rather than by juxtaposition of normal oceanic crust with only differences in age (e.g. Stern and Bloomer, 1992). Recent work on the intra-oceanic Tonga-Kermadec system, amongst the most robust subduction systems today, also suggests that it initiated at the site of an earlier subduction boundary (Sutherland et al., 2010). Another point of comparison is the Gagua Ridge, a relic compressional structure in the Philippine Sea, where seismic refraction images reveal oceanic crust of the West Philippine Basin underthrust beneath oceanic crust of the Huatung Basin, but the resultant Gagua Ridge became inactive and failed to develop into a subduction zone (Eakin et al., 2015). A final example of intra-oceanic subduction initiation is the Hjort trench, a zone of compression across an oceanic transform boundary, with seismic thrust faulting focal mechanisms and adjacent seamounts which may mark subduction initiation (Meckel et al., 2003). Further work is required to definitively determine general conditions for subduction initiation, but the resolution of crustal and lithospheric structure in a subduction zone, with precisely known plate kinematics during the nucleation phase, now provides the basis for a new generation of observationally constrained four-dimensional geodynamic models of the initiation process.

Acknowledgements

Supported by the National Science Foundation through awards OCE-1654766 (to Caltech) and OCE-1654689 (to UT Austin). We thank the Captain and crew of the R/V Marcus G. Langseth and S. Saustrup, M. Davis and D. Duncan from UTIG for their exceptional effort during the expedition. We thank T. Gerya for a helpful review of an earlier version of our manuscript. All seismic data will be made available at the Academic Seismic Portal (ASP) at UTIG while all remaining data will be available at the Rolling Deck to Repository (R2R). This is UTIG Contribution #3455.

Appendix A. Supplementary material

Supplementary material related to this article can be found online at https://doi.org/10.1016/j.epsl.2019.05.044.

References

Arculus, R.J., Ishizuka, O., Bogus, K.A., Gurnis, M., Hickey-Vargas, R., Aljahdali, M.H., Bandini, A.N., Barth, A.P., Brandl, P.A., Drab, L., do Monte Guerra, R., Hamada, M., Jiang, F., Kanayama, K., Kender, S., Kusano, Y., Li, H., Loudin, L.C., Maffione, M., Marsaglia, K.M., McCarthy, A., Meffre, S., Morris, A., Neuhaus, M., Savov, I.P., Sena, C., Tepley III, F.J., van der Land, C., Yogodzinski, G.M., Zhang, Z., 2015. A record of spontaneous subduction initiation in the Izu-Bonin-Mariana arc. Nat. Geosci. 8, 728–733.

Brocher, T.M., 2005. Empirical relations between elastic wavespeeds and density in the Earth's crust. Bull. Seismol. Soc. Am. 95, 2081–2092.

Cande, S.S., Stock, J.M., 2004. Pacific-Antarctic-Australia motion and the formation of the Macquarie Plate. Geophys. J. Int. 157, 399–414.

Christoffel, D.A., van der Linden, W.J.M., 1972. Macquarie Ridge-New Zealand Alpine fault transition. Antarct. Res. Ser. 19, 235–242.

Clarke, G.L., Klepeis, K.A., Daczko, N.R., 2000. Cretaceous high-P granulites at Milford Sound, New Zealand: metamorphic history and emplacement in a convergent margin setting. J. Metamorph. Geol. 18, 359–374.

Collot, J.-Y., Lamerche, G., Wood, R.A., Delteil, J., Sosson, M., Lebrun, J.-F., Coffin, M.F., 1995. Morphostructure of an incipient subduction zone along a transform plate boundary: Puysegur ridge and trench. Geology 23, 519–522.

Croon, M.B., Cande, S.C., Stock, J.M., 2008. Revised Pacific-Antarctic plate motions and geophysics of the Menard Fracture Zone. Geochem. Geophys. Geosyst. 9.

Davey, F., 2005. A Mesozoic crustal suture on the Gondwana margin in the New Zealand region. Tectonics 24.

Delteil, J., Collot, J.-Y., Wood, R., Herzer, R., Calmant, S., Christoffel, D., Coffin, M., Ferriere, J., Lamarche, G., Lebrun, J.-F., Mauffret, A., Pontoise, B., Popoff, M., Ruellan, E., Sosson, M., Sutherland, R., 1996. From strike-slip faulting to oblique subduction: a survey of the Alpine Fault-Puysegur trench transition, New Zealand, Results of Cruise Geodynz-sud Leg2. Mar. Geophys. Res. 18, 383–399.

DeMets, C., Gordon, R.G., Argus, D.F., 2010. Geologically current plate motions. Geophys. J. Int. 181, 1–80.

Dymkova, D., Gerya, T., 2013. Porous fluid flow enables oceanic subduction initiation on Earth. Geophys. Res. Lett. 40, 5671–5676.

Eakin, D.H., McIntosh, K.D., Van Avendonk, H.J.A., Lavier, L., 2015. New geophysical constraints on a failed subduction initiation: the structure and potential evolution of the Gagua Ridge and Huatung Basin. Geochem. Geophys. Geosyst. 16, 380–400.

Eberhart-Philips, D., Reyners, M., 2001. A complex, young subduction zone imaged by three-dimensional seismic velocity. Geophys. J. Int. 146, 731–746.

Escartin, J., Hirth, G., Evans, B., 1997. Nondilatant brittle deformation of serpentinites: implications of Mohr-Coulomb theory and the strength of faults. J. Geophys. Res. 102, 2897–2913.

Granot, R., Dyment, J., 2018. Late Cenozoic unification of East and West Antarctica. Nat. Commun. 9.

Gurnis, M., Hall, C., Lavier, L., 2004. Evolving force balance during incipient subduction. Geochem. Geophys. Geosyst. 5.

Gurnis, M., Yang, T., Cannon, J., Turner, M., Williams, S., Flament, N., Müller, R.D., 2018. Global tectonic reconstructions with continuously deforming and evolving rigid plates. Comput. Geosci. 116, 32–41.

Hayes, D.E., Talwani, M., 1972. Geophysical investigations of the Macquarie Ridge complex. In: Hayes, D.E. (Ed.), Antarctic Oceanology II: The Australian-New Zealand Sector. Am. Geophys. Un., Washington, D.C., pp. 211–234.

House, M.A., Gurnis, M., Kamp, P.J.J., Sutherland, R., 2002. Uplift in the Fiordland region, New Zealand: implications for incipient subduction. Science 297, 2038–2041.

Ishizuka, O., Kimura, J.-I., Li, Y.B., Stern, R.J., Reagan, M.K., Taylor, R.N., Ohara, Y., Bloomer, S.H., Ishii, T., Hargrove, U.S., Haraguchi, S., 2006. Early stages in the evolution of Izu-Bonin arc volcanism: new age, chemical, and isotopic constraints. Earth Planet. Sci. Lett. 250, 381–401.

Keller, W.R., 2003. Cenozoic Plate Tectonic Reconstructions and Plate Boundary Processes in the Southwest Pacific. Caltech, Pasadena.

Klingelhoefer, F., Biari, Y., Sahabi, M., Aslanian, D., Schnabel, M., Matias, L., Benabdellouahed, M., Funck, T., Gutscher, M.-A., Reichert, C., Austin, J.A., 2016. Crustal structure variations along the NW-African continental margin: a comparison of new and existing models from wide-angle and reflection seismic data. Tectonophysics 674, 227–252.

Lamarche, G., Lebrun, J.-F., 2000. Transition from strike-slip faulting to oblique subduction: active tectonics at the Puysegur margin, south New Zealand. Tectonophysics 316, 67–89.

Lamarche, G., Collot, J.-Y., Wood, R.A., Sosson, M., Sutherland, R., Delteil, J., 1997. The Oligocene-Miocene Pacific-Australia plate boundary, south of New Zealand: evolution from oceanic spreading to strike-slip faulting. Earth Planet. Sci. Lett. 148, 129–139.

Lebrun, J.-F., Karner, G.D., Collot, J.-Y., 1998. Fracture zone subduction and reactivation across the Puysegur ridge/trench system, southern New Zealand. J. Geophys. Res. 103, 7293–7313.

Leng, W., Gurnis, M., 2015. Subduction initiation at relic arcs. Geophys. Res. Lett. 42, 7014–7021.

Ludwig, W.J., Nafe, J.E., Drake, C.L., 1970. Seismic refraction. In: Maxwell, A.E. (Ed.), The Sea. Wiley-Interscience, New York, pp. 53–84.

Malatesta, C., Gerya, T., Crispini, L., Federico, L., Capponi, G., 2013. Oblique subduction modelling indicates along-trench tectonic transport of sediments. Nat. Commun. 4.

Mao, X., Gurnis, M., May, D.A., 2017. Subduction initiation with vertical lithospheric heterogeneities and new fault formation. Geophys. Res. Lett. 44.

Massell, C., Coffin, M.F., Mann, P., Mosher, S., Frohlich, C., Duncan, C.S., Karner, G., Ramsay, D., Lebrun, J.-F., 2000. Neotectonics of the Macquarie Ridge Complex, Australia-Pacific plate boundary. J. Geophys. Res. 105, 13457–13480.

McDermott, K., Reston, T., 2015. To see, or not to see? Rifted margin extension. Geology 43, 967–970.

McIntosh, K., Lavier, L., van Avendonk, H., Lester, R., Eakin, D., Liu, C.-S., 2014. Crustal structure and inferred rifting processes in the northeast South China Sea. Mar. Pet. Geol. 58B, 612–626.

McKenzie, D.P., 1977. The initiation of trenches: a finite amplitude instability. In: Talwani, M., Pitman, W.C. (Eds.), Island Arcs Deep Sea Trenches and Back-Arc Basins. Am. Geophys. Un., Washington, pp. 57–61.

Meckel, T.A., Coffin, M.F., Mosher, S., Symonds, P., Bernardel, G., Mann, P., 2003. Underthrusting at the Hjort Trench, Australian-Pacific plate boundary: incipient subduction? Geochem. Geophys. Geosyst. 4, 1099. https://doi.org/10.1029/2002GC000498.

Melhuish, A., Sutherland, R., Davey, F.J., Lamarche, G., 1999. Crustal structure and neotectonics of the Puysegur oblique subduction zone, New Zealand. Tectonophysics 313, 335–362.

Mitchell, J.S., Mackay, K.A., Neil, H.L., Mackay, E.J., Pallentin, A., Notman, P., 2012. Undersea New Zealand, 1:5,000,000, Chart, Miscellaneous Series 92 ed. NIWA.

Mortimer, N., Gans, P.B., Foley, F.V., Turner, M.B., Daczko, N., Robertson, M., Turnbull, I.M., 2013. Geology and age of Solander Volcano, Fiordland, New Zealand. J. Geol. 121, 475–487.

Mortimer, N., Tulloch, A.J., Spark, R.N., Walker, N.W., Ladley, E., Allibone, A., Kimbrough, D.L., 1999. Overview of the Median Batholith, New Zealand: a new interpretation of the geology of the Median Tectonic Zone and adjacent rocks. J. Afr. Earth Sci. 29, 257–268.

Nikolaeva, K., Gerya, T.V., Marques, F.O., 2010. Subduction initiation at passive margins: numerical modeling. J. Geophys. Res. 115.

Niu, Y., O'Hara, M.J., Pearce, J.A., 2003. Initiation of subduction zones as a consequence of lateral compositional buoyancy contrast within the lithosphere: a petrological perspective. J. Petrol. 144, 851–866.

Portner, R.A., Murphy, M.J., Daczko, N.R., 2011. A detrital record of lower oceanic crust exhumation within a Miocene slow-spreading ridge: Macquarie Island, Southern Ocean. Bull. Geol. Soc. Am. 123, 255–273.

Quilty, P.G., Crundwell, M.P., Wise, S.W., 2008. Microplankton provide 9 Ma age for sediment in the Macquarie Island ophiolite complex. Aust. J. Earth Sci. 55, 1119–1125.

Reagan, M.K., Pearce, J.A., Petronotis, K., Almeev, R.R., Avery, A.J., Carvallo, C., Chapman, T., Christeson, G.L., Ferré, E.C., Godard, M., Heaton, D.E., Kirchenbaur, M., Kurz, W., Kutterolf, S., Li, H., Li, Y., Michibayashi, K., Morgan, S., Nelson, W.R., Prytulak, J., Python, M., Robertson, A.H.F., Ryan, J.G., Sager, W.W., Sakuyama, T., Shervais, J.W., Shimizu, K., Whattam, S.A., 2017. Subduction initiation and ophiolite crust: new insights from IODP drilling. Int. Geol. Rev. 59, 1439–1450.

Reston, T.J., Pérez-Gussinyé, M., 2007. Lithospheric extension from rifting to continental breakup at magma-poor margins: rheology, serpentinisation and symmetry. Int. J. Earth Sci. 96, 1033–1046.

Reston, T.J., Ruoff, O., McBride, J.H., Ranero, C.R., White, R.S., 1996. Detachment and steep normal faulting in Atlantic oceanic crust west of Africa. Geology 24, 811–814.

Sandwell, D.T., Smith, W.H.F., 1997. Marine gravity anomaly from ERS-1, Geosat and satellite altimetry. J. Geophys. Res. 102, 10039–10045.

Schuur, C.L., Coffin, M.F., Frohlich, C., Massell, C.G., Karner, G.D., Ramsay, D., Caress, D.W., 1998. Sedimentary regimes at the Macquarie Ridge Complex: interaction of Southern Ocean circulation and plate boundary bathymetry. Paleoceanography 13, 646–670.

Stern, R.J., 2004. Subduction initiation: spontaneous and induced. Earth Planet. Sci. Lett. 226, 275–292.

Stern, R.J., Bloomer, S.H., 1992. Subduction zone infancy: examples from the Eocene Izu-Bonin-Mariana and Jurassic California arcs. Geol. Soc. Am. Bull. 104, 1621–1636.

Sutherland, R., 1995. The Australia-Pacific boundary and Cenozoic plate motions in the SW Pacific: some constraints from Geosat data. Tectonics 14, 819–831.

Sutherland, R., Melhuish, A., 2000. Formation and evolution of the Solander Basin, southwestern South Island, New Zealand, controlled by a major fault in continental crust and upper mantle. Tectonics 19, 44–61.

Sutherland, R., Barnes, P., Uruski, C., 2006. Miocene-Recent deformation, surface elevation, and volcanic intrusion of the overriding plate during subduction initiation, offshore southern Fiordland, Puysegur margin, southwest New Zealand. N.Z. J. Geol. Geophys. 49, 131–149.

Sutherland, R., Collot, J., Lafoy, Y., Logan, G.A., Hackney, R., Stagpoole, V., Uruski, C., Hashimoto, T., Higgins, K., Herzer, R.H., Wood, R., Mortimer, N., Rollet, N., 2010. Lithosphere delamination with foundering of lower crust and mantle caused permanent subsidence of New Caledonia Trough and transient uplift of Lord Howe Rise during Eocene and Oligocene initiation of Tonga-Kermadec subduction, western Pacific. Tectonics 29, 1–16.

Sutherland, R., Davey, F., Beavan, J., 2000. Plate boundary deformation in South Island, New Zealand, is related to inherited lithospheric structure. Earth Planet. Sci. Lett. 177, 141–151.

Sutherland, R., Gurnis, M., Kamp, P.J.J., House, M.A., 2009. Regional exhumation of brittle crust during subduction initiation, Fiordland, southwest New Zealand: implications for thermochronologic sampling and analysis strategies. Geosphere 5, 409–425.

Thielmann, M., Kaus, B.J.P., 2012. Shear heating induced lithospheric-scale localization: does it result in subduction? Earth Planet. Sci. Lett. 359–360, 1–13.

Toth, J., Gurnis, M., 1998. Dynamics of subduction initiation at pre-existing fault zones. J. Geophys. Res. 103, 18053–18067.

Van Avendonk, H.J.A., Davis, J.K., Harding, J.L., Lawver, L.A., 2017. Decrease in oceanic crustal thickness since the breakup of Pangaea. Nat. Geosci. 10, 58–61.

Walcott, R.I., 1998. Modes of oblique compression: late Cenozoic tectonics of the South Island of New Zealand. Rev. Geophys. 36, 1–26.